central zone, as well as the faults that had movement at the surface, can be interpreted as part of a basin-and-range fault system that extends under Pahute Mesa from the eastern side of Gold Flat, which is north of the mesa. Immediately south of Pahute Mesa, the fault system is obliterated by younger volcanic structures and rocks. The east-trending zone of epicenters 3.5 km south of ground zero nearly coincides with the exposed edge of the Timber Mountain caldera. These epicenters may have been controlled by the outermost ring fractures of the caldera.

Although some fracturing occurred within the zone of epicenters, the major movements were located to the east of it. Some understanding of this apparently rather puzzling relation can be gained by considering the distribution of the depth of the earthquakes together with the geologic structure (Fig. 2).

The focal depths of the earthquakes ranged from near zero to approximately 6 km. Most of the foci in the eastern part of the seismic region are in the depth range 1 to 4 km. In the western part the depths reach 6 km. Northwest of ground zero the seismic zone dips about 45°NW. This part of the seismic zone may correlate with the boundary of the Silent Canyon Caldera (*12*). Probably all hypocenters (Fig. 2) are within volcanic rocks despite the queried contact between older volcanic rocks and granite or metamorphic rocks. A drill hole (UE20f) 4170 m deep in the vicinity of these hypocenters bottomed in volcanic rock, and it is estimated that at least another 1000 m of volcanic rock occurs below the bottom of the hole (*13*). To the southwest, the zone is essentially vertical to a depth of 6 km. The earthquakes in this region may define the extension under the younger volcanic rocks of the north-trending fault that lies to the south (Fig. 1) and appears to lead into the seismic trend.

These findings suggest that the Benham explosion initiated movement along previously existing geologic boundaries. Movement at the surface occurred mainly along faults east of ground zero and was not associated with significant earthquake activity. West of the faulting, earthquakes occurred to about the depth of basement; farther west they define dipping zones that may correlate with similarly dipping basin-and-range structure. The tendency of some of the earthquakes to be aligned along parts of caldera boundaries and for nearly all of the earthquakes to be in volcanic rocks within a caldera seems to imply a genetic relationship. Additional information and study are required, however, to confirm the exact relationship.

We conclude that the seismic activity and the fault movement result primarily from the release of natural tectonic strain initiated by the explosion. The lack of radial symmetry in the distribution of epicenters, the pattern of *P*-wave first motions, and the correlation with preexisting geologic structures support this conclusion. In addition, the consistent northwest to southeast directions for the tension axes determined from the fault-plane solutions are in agreement with the direction of extension found for the earthquake near Fairview Peak in central Nevada (*14*) and with the extension direction indicated by the Raleigh wave radiation pattern produced by the Hardhat explosion in Yucca Flat at the Nevada Test Site (*7*).

R. M. HAMILTON
*U.S. Geological Survey,*
*Menlo Park, California 94025*
F. A. MCKEOWN
*U.S. Geological Survey,*
*Denver, Colorado 80225*
J. H. HEALY
*U.S. Geological Survey,*
*Menlo Park, California 94025*

### References and Notes

1. R. B. Hoy, *Bull. Seismol. Soc. Amer.* **53**, 845 (1963).
2. D. D. Dickey, F. A. McKeown, W. L. Ellis, *Technical Letter: Special Studies—65, U.S. Geol. Surv. Open File Report* (1968).
3. D. D. Dickey, E. C. Jenkins, F. A. McKeown, W. H. Lee, *Technical Letter: NTS-196, U.S. Geol. Surv. Open File Report* (1967); D. D. Dickey, *Geol. Soc. Amer. Mem.* **110**, 219 (1968); F. A. McKeown, D. D. Dickey, W. L. Ellis, *Technical Letter: Central Nevada-16, U.S. Geol. Surv. Open File Report* (1968).
4. W. H. Westphal, *Stanford Res. Inst. Final Rep. VUP-0607, Project 7.6* (1962); *Stanford Res. Inst. Tech. Rep. 6, Project 7.6* (1964).
5. F. Press and C. Archambeau, *J. Geophys. Res.* **67**, 337 (1962).
6. J. N. Brune and P. W. Pomeroy, *ibid.* **68**, 5005 (1963).
7. M. N. Toksöz, A. Ben-Menahem, D. G. Harkrider, *ibid.* **70**, 907 (1965).
8. G. Boucher, A. Ryall, A. E. Jones, *ibid.* **74**, 3808 (1969).
9. J. F. Evernden, *Trans. Amer. Geophys. Union* **50**, 247 (1969).
10. A. Ryall and W. U. Savage, *J. Geophys. Res.* **74**, 4281 (1969).
11. One of the earthquakes beyond 13 km was located 22 km northwest of ground zero and the other two were 21 km southeast. All three earthquakes occurred during the second week after the explosion.
12. P. P. Orkild, F. M. Byers, Jr., D. L. Hoover, K. A. Sargent, *Geol. Soc. Amer. Mem.* **110**, 77 (1968).
13. P. P. Orkild, personal communication.
14. L. J. Meister, R. O. Burford, G. A. Thompson, R. L. Kovach, *J. Geophys. Res.* **73**, 5981 (1968).
15. Mapping aspects supported by U.S. Atomic Energy Commission.

20 August 1969

## Freshwater Ferromanganese Concretions: Chemistry and Internal Structure

Abstract. *Studies by optical microscopy, x-ray diffraction, and electron probe techniques of ferromanganese concretions from three Canadian lakes reveal chemical banding of amorphous hydrated iron and manganese oxides. The average ratio of iron to manganese in concretions from these lakes varies from 0.43 to 2.56. The concentrations of cobalt, nickel, copper, and lead are one to two orders of magnitude below those reported for oceanic ferromanganese concretions.*

Freshwater ferromanganese concretions have been observed in small lakes in eastern Canada, Scandinavia, western Russia, northern England, and New England, and in the Great Lakes (*1–3*). Thus far there have been no reported occurrences of ferromanganese concretions in freshwater environments in subtropical or tropical regions. This report presents the results of the first detailed study on the mineralogy, internal structure, and chemistry of freshwater ferromanganese concretions from Canadian lakes.

The presence of ferromanganese concretions in Canadian lakes has been reported by Honeyman (*4*) and by Kindle (*5*). Concretions for this study were collected from Grand Lake and Ship Harbour Lake, Nova Scotia, and Mosque Lake, Ontario. The geological environment of these lakes is very different, with the Nova Scotia lakes being developed on sedimentary rocks of different ages and the Ontario lake overlying biotitic gneisses. All of the concretions discussed here were collected in 0.5 to 2.0 m of water. The substrate at all the concretion sites visited consisted of coarse-grained quartz sand and pebbles. The ferromanganese precipitate forms on a pebble nucleus and always exhibits a maximum thickness in a zone 0.5 to 3.0 cm above the sediment-water interface. The nuclei for concretion formation include slate, sandstone, and granite pebbles. No particular type of rock seems to be preferred for nucleation. The morphology of ferromanganese concretions in Canadian lakes varies from bands of precipitate which grow parallel to the sediment-water interface to nodular concretions where ferromanganese oxide completely encloses the rock nucleus.

Examination of the ferromanganese precipitate by optical, x-ray diffraction, and x-ray powder diffraction techniques with the use of both unfiltered and manganese-filtered iron x-radiation demonstrated a total absence of any crystalline ferromanganese minerals. Detrital grains of quartz and oligoclase feldspar were identified as contaminants in the ferromanganese precipitate. These minerals are major constituents in bottom sediments associated with the concretions.

Analytical data on the major and trace elements in ferromanganese precipitates from the three Canadian lakes are presented in Table 1. Iron and Mn were determined by x-ray fluorescence; Co, Ni, Cu, Zn, and Pb were determined by atomic absorption. The samples are numbered to indicate the lake, the site within that lake, and the specimen analyzed; for example, sample number GL-1-W indicates specimen W, collected from site 1 in Grand Lake, Nova Scotia. Specimens which were analyzed in duplicate are indicated by the inclusion of the letter A or B after the specimen number. The analysis of composite samples is indicated by the inclusion of the letter C followed by the sample number, and the number of concretions in the composite is given in parentheses. The ratio of Fe to Mn (Table 1) varies from 0.43 to 2.56. Precipitates from the two Nova Scotia lakes exhibit a similar composition of major elements and have lower ratios of Fe to Mn than usual in freshwater concretions (*6*). The Mosque Lake concretions exhibit ratios of Fe to Mn approximately five times larger than precipitates from the Nova Scotia lakes. The Co, Ni, and Zn contents of precipitates from all three lakes are distinct. A comparison of the average composition and range in composition of freshwater ferromanganese precipitates with the composition of oceanic precipitates from the Pacific given by Mero (*7*) indicates considerable overlap in the ratios of Fe to Mn and in Zn concentrations. The freshwater precipitates have Co, Ni, Cu, and Pb contents falling 1 to 2 orders of magnitude below the corresponding concentrations in oceanic ferromanganese precipitates. Similar results have been reported for ferromanganese precipitates from Swedish lakes (*3*) and the English Lake District (*2*).

The internal distribution of Fe and Mn was investigated by electron probe techniques. Figure 1 shows x-ray intensity profiles for Fe and Mn from a traverse across a 300-$\mu$m cross section of a sample from Grand Lake. The Fe and Mn contents of the concretion occur in distinct bands of variable thickness. Many of the bands that are rich in Fe and Mn are discontinuous as a result of abrasion caused by the movement of sediment over the concretions during storms and the periodic movement of nodules from one side to another. Ferromanganese precipitate deposited adjacent to the sediment surface by wave action dissolves. We observed concretions being buried under sediment during a storm at Mosque Lake and collected numerous samples with portions of circular concretion material missing as a result of dissolution of the ferromanganese precipitate which had been buried below the sediment surface.

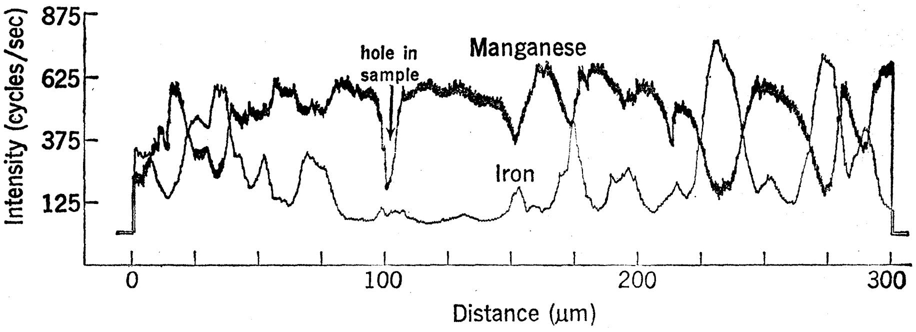

Fig. 1. Electron probe x-ray intensity profiles for Fe and Mn obtained from a traverse across a 300-$\mu$m cross section of a concretion from Grand Lake, Nova Scotia.

The two major features which must be taken into account in any theory for the origin of freshwater ferromanganese concretions are the limited geographic distribution of the concretions to temperate and subarctic environments and the presence of chemical banding. Other features of the ferromanganese precipitates, such as variations in the content of trace elements, are most likely a reflection of local watershed composition rather than the mechanism of formation.

We hypothesize that a pair of oxide bands, one Fe-rich and one Mn-rich, represents the annual growth increment of the ferromanganese concretions. Growth rates calculated on the basis of the foregoing assumption range from 0.1 mm/year in the Nova Scotia lakes to 1.5 mm/year in Mosque Lake. These accumulation rates are compatible with Kindle's (*5*) estimate based on the thickness of ferromanganese precipitates on human artifacts of approximate known age. This suggests that our initial assumption may be valid, and, if so, it provides a useful method for the determination of concretion age and

Table 1. Chemistry of concretions from Grand Lake (GL) and Ship Harbour Lake (SH), Nova Scotia, and Mosque Lake (ML), Ontario.

| Sample No. | Fe/Mn | Fe (% by weight) | Mn (% by weight) | Co (ppm) | Ni (ppm) | Cu (ppm) | Zn (ppm) | Pb (ppm) |
|---|---|---|---|---|---|---|---|---|
| GL-1-W | 0.433 | 15.5 | 35.9 | 220 | 338 | 13 | 1940 | 25 |
| GL-1-X | .599 | 20.9 | 34.9 | 202 | 243 | 12 | 1575 | 24 |
| GL-1-XA | .599 | 20.9 | 34.9 | 192 | 230 | 8 | 1500 | 28 |
| GL-1-Y | .552 | 18.6 | 33.7 | 192 | 215 | 10 | 1575 | 26 |
| GL-1-YA | .549 | 18.7 | 34.0 | 192 | 215 | 10 | 1575 | 26 |
| GL-1-Z | .577 | 19.3 | 33.4 | 192 | 215 | 10 | 1340 | 25 |
| GL-1-Cl (10) | .530 | 18.1 | 34.2 | 192 | 373 | 16 | 1850 | 26 |
| GL-1-C2 (10) | .549 | 17.8 | 32.4 | 202 | 272 | 16 | 1650 | 28 |
| GL-2-Y | .468 | 16.8 | 35.9 | | | | | |
| GL-2-Z | .434 | 14.6 | 33.6 | 212 | 373 | 14 | 1875 | 13 |
| GL-2-Cl (9) | .449 | 14.2 | 31.7 | 183 | 238 | 11 | 1575 | 28 |
| GL-2-ClB (9) | .449 | 14.2 | 31.7 | 192 | 238 | 10 | 1650 | 29 |
| GL-4-Z | .470 | 16.3 | 34.4 | | | | | |
| GL-4-Cl (5) | .457 | 14.7 | 32.2 | 202 | 316 | 13 | 1500 | 19 |
| SH-1-X | .458 | 11.7 | 25.5 | 230 | 125 | 9 | 536 | 19 |
| SH-1-Y | .709 | 20.0 | 28.3 | 230 | 149 | 8 | 500 | 19 |
| SH-1-Z | .560 | 15.7 | 28.1 | 212 | 149 | 8 | 518 | 28 |
| SH-1-ZA | .560 | 15.7 | 28.1 | 220 | 149 | 8 | 536 | 10 |
| SH-1-Cl (16) | .636 | 16.9 | 26.5 | 220 | 107 | 6 | 467 | 28 |
| ML-1-Z | 2.52 | 39.8 | 15.7 | | | | | |
| ML-1-Cl (16) | 2.56 | 40.2 | 15.7 | 135 | 95 | 10 | 250 | 24 |

growth rates. At the growth rates indicated, the largest nodules observed would have initiated growth approximately 1600 years ago. This could indicate a physical limit on concretion size at approximately 16 cm or a physicochemical change in lake conditions 1600 years ago. A detailed study of the ferromanganese bands in freshwater nodules could provide a new method for the interpretation of past hydrochemical conditions in lakes.

ROBERT C. HARRISS
*Oceanography Department,*
*Florida State University, Tallahassee*
ARTHUR G. TROUP
*Geology Department,*
*McMaster University,*
*Hamilton, Ontario*

### References and Notes

1. E. M. Kindle, *Amer. J. Sci.* **24**, 496 (1932); P. Ljunggren, *Geol. Foren. Stockholm Forh.* **75**, 277 (1953); R. Rossman and E. Callender, *Science* **162**, 1123 (1968).
E. Gorham and D. Swaine, *Limnol. Oceanogr.* **10**, 268 (1965).
3. F. T. Manheim, *Univ. Rhode Island Occas. Publ. No. 3-1965* (1965), p. 217.
4. D. Honeyman, *Proc. Trans. Nova Scotia Inst. Nat. Sci.* **5**, 328 (1881).
5. E. M. Kindle, *Econ. Geol.* **31**, 755 (1936).
6. N. B. Price, *Mar. Geol.* **5**, 511 (1967).
7. J. Mero, *The Mineral Resources of the Sea* (Elsevier, Amsterdam, 1965).
8. Supported by the National Research Council of Canada and Geological Survey of Canada. We thank D. Church, J. R. Kramer, and G. V. Middleton for comments, R. H. McNutt for assistance with the x-ray fluorescence analyses, and J. Grootenboer for assistance in preparation of polished sections for electron probe studies. Contribution No. 236, Department of Oceanography, Florida State University.

7 May 1969; revised 29 May 1969

---

## Particle Track Enhancement in Cellulose Nitrate by Application of an Electric Field

Abstract. *The number and length of etchable tracks, created by alpha particles in a cellulose nitrate sheet, are significantly enhanced by the application of an electric field across the cellulose nitrate.*

When a highly ionizing particle traverses a dielectric medium, it disrupts atomic and molecular structure along its path. Subsequent etching preferentially attacks this region of damage, thus causing the resulting track to become visible (*1*). We have observed enhancement of the damage created by low-energy alpha particles through the application of an electric field across the dielectric cellulose nitrate during the passage of the particle.

Two principal mechanisms, compatible with available data, have been suggested to explain the processes by which the track damage is created. Fleischer *et al.* (*2, 3*) have proposed a mechanism called the "ion explosion spike." According to this model, a highly ionizing particle leaves behind a small cone or cylinder of positively charged ions. If the ion density is sufficiently high, mutual Coulomb repulsion will eject the ions into the surrounding lattice. This leaves a region containing many dislocated atoms that is chemically reactive. However, this mechanism is not sufficient to explain etchable track formation by alpha particles in polymers. In a polymeric material such as cellulose nitrate, less energy is required to break the chemical bonds than to ionize the atoms. Hence it has been suggested (*2*) that the breaking and rearranging of the chemical bonds in polymeric materials contribute to the damage mechanism.

A second mechanism, proposed by Benton (*4*), suggests that delta-ray electrons, created by the passage of the ionizing particle, are responsible for the necessary damage. Molecular fragments, created by the delta rays, are then more soluble in the etchant than the unfragmented molecules of the dielectric.

The nature of the mechanism for energy loss in matter is such that many atoms, while receiving some energy from the passage of the ionizing particle, decay rapidly to the ground state with no permanent change in the material. If the excited atom is in an electric field, it is further perturbed because of the additional forces generated by the field. The application of an external electric field during the passage of the ionizing particle would then be expected to increase the number of atomic sites that have been permanently disrupted. It has been demonstrated (*2, 3*) that the specific ionization due to the incident particle must exceed a threshold value characteristic of the irradiated material in order to produce etchable tracks. It was anticipated, therefore, that it should be possible to use an externally impressed electric field to increase the damage and thereby enhance the production of etchable tracks.

We have examined the tracks created by alpha particles in cellulose nitrate. This polymer was chosen because it has a known threshold of specific ionization for the creation of tracks, corresponding to an alpha particle with an energy of 3 Mev. Alpha particles with energies greater than 3 Mev do not lose energy at a sufficient rate to leave etchable tracks in cellulose nitrate. We have used as a source of alpha particles $Po^{210}$ which emits a 5.3-Mev alpha particle. The experimental arrangement is shown in Fig. 1. The alpha particles pass through a thin region of air (*5*) and then through a high-voltage grid before they strike a sheet of cellulose nitrate 0.25 mm thick. If we vary the distance between the source and the cellulose nitrate, the energy attenuation due to the air can be controlled. The alpha particles penetrate the cellulose nitrate to a depth of approximately 25 $\mu$m. The electric field is created by applying voltage between the high-voltage grid and a grounded grid placed on the other side of the cellulose nitrate. We have made tests with external fields varying from 0 to $1.8 \times 10^5$ volt/cm. After the cellulose nitrate samples have been irradiated, the samples are etched in a 6*N* solution of NaOH at 25°C for 2 hours.

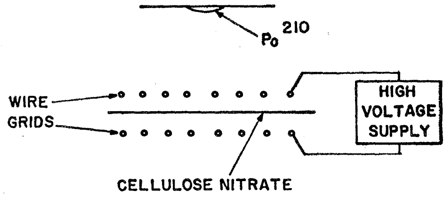

Fig. 1. Schematic view of the experimental apparatus used to enhance tracks created by alpha particles in cellulose nitrate.

The results reported here have been obtained with alpha particles which have passed through 1 cm of air. They strike the cellulose nitrate with an incident energy range of approximately 3.5 to 4.0 Mev. This spread in energy is due to variations in the path length of the alpha particles in air. As expected, in the absence of an electric field, alpha particles with an energy greater than 3.5 Mev do not create enough damage in cellulose nitrate to produce etchable tracks. However, when electric fields in excess of $6 \times 10^4$ volt/cm are applied, etched tracks become visible. We have attempted to estimate the efficiency of track formation by 4-Mev alpha particles in the presence of an electric field by comparing the number of tracks observed with those formed by 2.5-Mev alpha particles. With an external field of $10^5$ volt/cm the track formation efficiency of 4-Mev